Energetics and Structural Elucidation of Mechanisms for Gas Phase H/D Exchange of Protonated Peptides

ARTICLE *in* THE JOURNAL OF PHYSICAL CHEMISTRY A · OCTOBER 2010

Impact Factor: 2.69 · DOI: 10.1021/jp105170f · Source: PubMed

2 AUTHORS:

Blake E Ziegler
University of Waterloo
9 PUBLICATIONS **33** CITATIONS
SEE PROFILE

Terrance Mcmahon
University of Waterloo
206 PUBLICATIONS **5,443** CITATIONS
SEE PROFILE

Energetics and Structural Elucidation of Mechanisms for Gas Phase H/D Exchange of Protonated Peptides

Blake E. Ziegler and Terry B. McMahon*

Department of Chemistry University of Waterloo Waterloo, Ontario

Received: June 5, 2010; Revised Manuscript Received: September 19, 2010

Hydrogen/deuterium exchange reactions involving protonated triglycine and deuterated ammonia (ND_3) have been examined in the gas phase using a Fourier transform ion cyclotron resonance (FT-ICR) mass spectrometer. Ab initio and density functional theory (DFT) calculations have been carried out to model the exchanges and to obtain energetics and vibrational frequencies for molecules involved in the proposed exchange mechanisms. Structural optimization and frequency calculations have been performed at the B3LYP level of theory with the 6-311+G(d,p) basis set. Transition states have been calculated at the same level of theory and basis set as above using the QST2 and QST3 methods. Single-point energy calculations have been performed at the MP2/6-311+G(d,p) level. Six labile sites of protonated triglycine were found to undergo H/D exchange. Of these six labile hydrogens, two are amide, three are ammonium, and one is carboxyl. Detailed mechanisms for each of these transfers are proposed. Qualitative onium ion and tautomer mechanisms for the exchanges of ammonium and amide hydrogens, respectively, using semiempirical calculations were suggested in previous studies by Beauchamp et al. As shown by the current ab initio and DFT calculations completed during this study, the mechanisms proposed in that study are notionally correct; however, the tautomer mechanisms are shown here to be the result of the fact that a second stable isomer of protonated triglycine exists in which the amide1 carbonyl oxygen is protonated. The exchange of the carboxyl hydrogen is found to proceed via a transition state resembling an ammonium ion interacting with a carboxylate moiety via two hydrogen bonds. The current work thus provides significant mechanistic and structural detail for a considerably more in-depth understanding of the processes involved in gas phase H/D exchange of peptides.

Introduction

Hydrogen/deuterium (H/D) exchange has been used in numerous studies to probe protein folding, dynamics, conformational stability, and ligand binding, as well gas and solution phase structure, making it an effective tool in the investigation of proteins.

For short polypeptides, deuterated solvent can relatively easily access all of the labile hydrogen sites resulting in exchange at all possible sites. For longer polypeptides, extensive folding may occur, and as a result of intramolecular interactions, otherwise labile hydrogen sites become difficultly accessible to the solvent, with the consequence that exchange at these sites occurs much more slowly or not at all. The different rates of exchange at the labile sites, as well as the number of exchanged sites, can thus give information about the peptide.

H/D exchange has been used in experiments to probe protein folding.[1] Parker and Clarke examined the folding of an all-beta domain of the cell adhesion molecule, CD2, in rat, and found that it folds through an intermediate that is rapidly formed.[2] Nishimura and co-workers have also used H/D exchange to further understanding of protein folding, investigating the structure of intermediates in the apomyoglobin folding pathway.[3] The folding pathway of apomyoglobin was further investigated by Uzawa et al. using 2D NMR.[4]

H/D exchange can also be used in the study of protein unfolding. This has been shown by Mobley and Poliakov in an exchange experiment involving the dimer protein, *Bacillus subtilis* NAD^+ synthetase. H/D exchange proved that the dimer undergoes a reversible dissociation into unfolded monomeric subunits at increased temperatures, allowing for the proposition of an unfolding model for this protein.[5]

In the analysis of protein dynamics, Maity and co-workers investigated the replacement of lysine with glycine in a helix of cytochrome *c*, finding that although the native structure of the protein remains unchanged, its flexibility is increased, which could possibly promote unfolding.[6]

The conformational stability of proteins can also be explored using H/D exchange.[7] Wang and Tang used the technique to assess the stability of apomyoglobin in solution and found that both the native and intermediate conformations have dynamic strucutures.[8] Finally, a fairly recent technique denoted SUPREX (stability of unpurified proteins from rates of H/D exchange) uses H/D exchange to evaluate the stability of proteins in solution.[9]

Importantly, H/D exchange can also give insight into protein−ligand interactions applicable to enzymatic research. Wang and co-workers investigated wild-type Yersinia protein tyrosine phosphatase in the presence of its competitive inhibitor, vanadate, to further understanding on how the binding of vanadate affects the protein conformation.[10] As well, a thorough review exists on the subject of enzymatic research utilizing H/D exchange to study ligand binding, protein−protein interactions, and protein activation by modification.[11]

Interestingly, H/D exchange has also been used in the study of proteins embedded in lipid bilayers[12,13] and structural studies on proteins implicated in various diseases, such as β(2)-microglobulin amyloid fibrils that cause amyloidosis[14] and prions that cause Creutzfeldt-Jakob disease, among others.[15−17]

* Corresponding author. E-mail: mcmahon@uwaterloo.ca.

10.1021/jp105170f
Published on Web 10/18/2010

As shown above, the majority of studies concerning H/D exchange involve reactions carried out in the solution phase with peptides that are subsequently analyzed using NMR spectroscopy[18−21] or mass spectrometry.[22] However, much less work has been carried out to elucidate the structures of proteins and peptides in the gas phase.

Gas phase H/D exchange behavior of proteins is useful because it permits insight into the intrinsic interactions of a protein in the absence of a solvent. An early study of H/D exchange by Cheng and Fenselau involved leucine enkephalin and leucine enkephalin−arginine and ND_3. They found that H/D exchange rates and the number of exchanged hydrogens is dependent on proton affinity of the protonated peptides, collision energy, and the solvent gas pressure.[23] Gard and co-workers investigated the reactions of deuterated methanol with protonated amino acids and their esters, leading them to propose that the gas phase basicity difference between the amino acids and the solvent gas has an effect on H/D exchange.[24,25] Wood et al. experimented with cations of cytochrome *c* and determined that removing water from a peptide may induce its folding.[26] A mechanism for the H/D exchange of gas phase peptides with heavy water was proposed by Wyttenbach and Bowers from a study of protonated bradykinin.[27] Rozman independently performed an experiment with supporting DFT calculations involving the H/D exchange of protonated amino acids and their esters with deuterated water and methanol.[28] Some mechanisms of exchange were suggested. Most recently, the H/D exchange of potassiated tryptophan was investigated by Polfer et al., who found that some ions adopting a zwitterion structure are evident postexchange.[29]

As well, sodiated peptides have been examined through H/D exchange in studies by various groups, and it has been discovered that sodiated polyglycines up to Gly5 only undergo three exchanges, possibly suggesting that two of the labile hydrogens are amino and one is carboxyl, implying that the amide exchanges are the least favorable.[30,31]

Relatively little work has been carried out on the determination of protein and peptide structure in the gas phase; thus, few research groups have studied the mechanisms of exchange of the labile hydrogen atoms in the gas phase.

A significant advance in the mechanistic study of gas phase H/D exchange with mass spectrometry was made by Beauchamp and co-workers, who examined the H/D exchange reactions of a series of protonated oligomers of glycine, consisting of 1−5 subunits, with each of D_2O, CD_3OD, CD_3COOD, or ND_3 at low pressure in a FT-ICR cell.[32] It was found that ND_3 was the sole solvent molecule of the series that permitted complete exchange of all possible labile hydrogens for each of the oligomers. The underlying reason advanced for the more favorable and complete exchange with ND_3 was associated with the much greater gas phase basicity of ammonia relative to the other compounds, allowing for a smaller gas phase basicity difference between the molecules, which permitted proton transfer from the peptide to ammonia within an ion−molecule complex.

These authors also proposed that the subsequent exchanges of protonated triglycine and ND_3 could be explained by three separate mechanisms, which were supported by AM1 and PM3 semiempirical calculations. The first of these mechanisms, implicated in exchange in protonated peptides, was an onium ion mechanism to explain the three possible protonated amine terminus exchanges. This involves the deprotonation of the protonated amine group and the subsequent solvation of an ND_3H^+ onium ion by the neutral polypeptide via a $N\cdots H^+\cdots N$ strong hydrogen bond. Following the solvation of this onium ion, a rotation of the ND_3H^+ group would allow the back-transfer of a deuteron to the amine terminus. A tautomer mechanism was suggested to explain the amide exchanges in which the carbonyl of the amide group is protonated, allowing a hydrogen of the amide nitrogen to be removed by ND_3 to form ND_3H^+. As above, this onium ion could then transfer a deuteron back to the amide nitrogen, followed by a deprotonation of the amide carbonyl. Finally, the exchange of the labile hydroxyl of the peptide C-terminal carboxyl group requires transfer of the carboxyl hydrogen to ND_3 and the subsequent stabilization of ND_3H^+ by the resulting anionic carboxylate group. Rotation of ND_3H^+ and transfer of D^+ then leads again to an exchange. Quantitative structural details were not provided; neither were transition states located on the potential energy surface.

Recent work from our laboratory has involved new FTICR observations of H/D exchange for the series of polyglycines up to Gly8. In the current study, ab initio and DFT electronic structure calculations have been used to determine the structures of the protonated triglycine as well as the possible complexes with ammonia to determine mechanisms for the exchange reaction with computational location of key transition states on the potential energy surface. From this experimental and computational combination, it has been possible to propose new mechanisms for the exchange of each of the types of labile hydrogen in the protonated species. Protonated triglycine has been used as a prototypical model for gas phase peptide analysis, since it contains the several different types of exchangeable hydrogen: i.e., amine terminus, carboxyl terminus, and two distinctly different amide locations. As well, the polypeptide is large enough to give an accurate representation of a naturally occurring peptide without being too large and, thus, computationally expensive for high level ab initio and DFT calculations. Protonated betaine has also been studied to gain further insight into the carboxyl proton exchange mechanism. As described below, although qualitative similarities exist between the detailed mechanisms determined here and those obtained by the semiempirical methods used by Beauchamp and co-workers, there are some significant differences both in the structures involved and energetics obtained. Notably, the two amide exchange mechanisms are substantially different. In addition, all relevant transition states have been located.

Experimental and Computational Methods

Gas phase H/D exchange experiments were carried out on a Bruker BioAPEX III Fourier-transform ion cyclotron resonance mass spectrometer with a 7 T magnet which has been described in detail elsewhere.[33] The pressure of ND_3 in the FTICR cell was determined via calibration of the ionization gauge reading using well-known reaction rate constants for ion−molecule reactions involving ammonia, as well as other species. The walls of the vacuum system were conditioned by repetitive additions and evacuations of ND_3 in the FT-ICR cell and inlet lines. Each of the protonated polyglycines was generated by electrospray ionization and then accumulated in an rf-only quadrupolar field before being transferred as a pulse to the FT-ICR cell via a series of high voltage ion optical elements. The reactant ions are decelerated to ≤ 1 eV by a cylindrical decelerator lens assembly in the fringing field of the superconducting magnet and then trapped in the FTICR cell, following which any excess kinetic energy was removed by a pulse of Ar gas into the cell to effect efficient collisional cooling. The protonated species of interest was then isolated in the FTICR cell by a series of rf

ejection events and allowed to react with the ND_3 at pressures between 5×10^{-9} and 5×10^{-8} mbar, depending upon the magnitude of the exchange rate constants. Mass spectra were then taken at a series of controlled delay times spaced at relatively short intervals in the early reaction period to much longer intervals later in the reaction sequence when overall relative intensities were changing much more slowly.

Ab initio calculations were performed using the Gaussian 03 program package.[34] The B3LYP[35] level of theory with a 6-311+G(d,p) basis set was used for structural optimizations and frequency calculations. This level of theory and basis set has been proven to be a relatively low computational cost yet high accuracy method of calculating vibrational frequencies[36,37] and optimized structures for complexes which exhibit hydrogen bonding.[38] Single point energy calculations were subsequently carried out at the MP2/6-311+G(d,p) level. Single point energy calculations at this level of theory and basis set have been shown to generally be closer to experiment than energetics calculated with the same basis set at the B3LYP level of theory. Transition states were calculated using the QST2 and QST3 methods and verified by identification of a single imaginary frequency. No basis set superposition error correction was applied to the results, since it has been proven that high-level, single point energy calculations correlate more accurately with experiment without any correction.[39] All mechanistic deductions below have been made using energetics determined at the MP2/6-311+G(d,p) level. As well, the potential energy surfaces depicted list energetics calculated at 0 K without inclusion of zero-point energies to allow facile depiction of transition states.

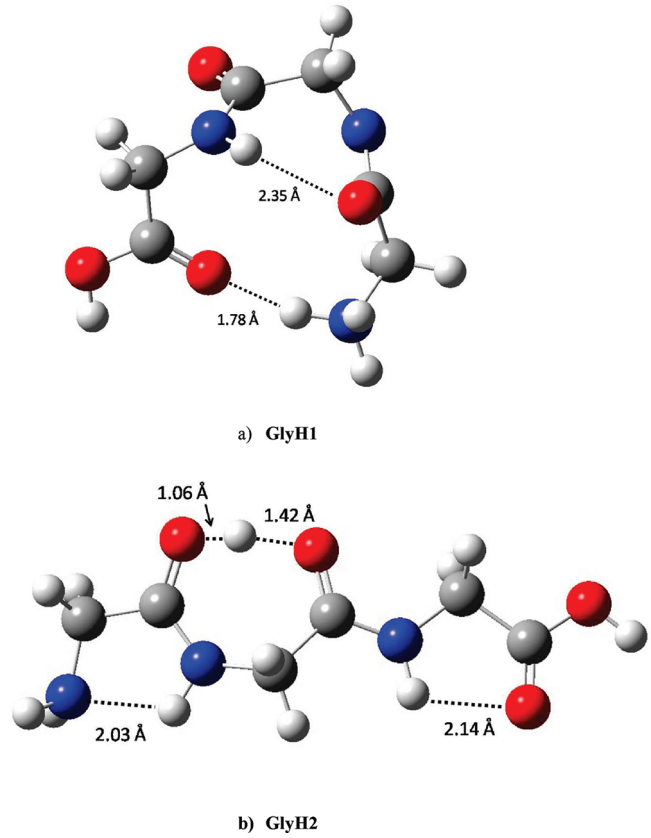

Figure 1

Results and Discussion

As Beauchamp et al. have previously shown, gas phase H/D exchange of protonated polyglycines, from Gly3 to Gly5 with ND_3, leads to exchange of all labile hydrogens, with the number of exchanges increasing with increasing peptide chain length. In the current study, H/D exchange experiments were carried out for polyglycines ranging from Gly3 to Gly8. The results mimic those generally observed by Beauchamp et al. For purposes of elucidation of the H/D exchange mechanisms, protonated triglycine has been used as a model system as it has each of the important different types of labile hydrogen; that is, protonated amine of the N-terminus, hydroxyl hydrogen of the carboxyl C-terminus, and hydrogens on the amide nitrogens. In addition, protonated triglycine has been shown previously to have two forms, very close in energy, which represent the different possibilities in each of the higher-order protonated polyglycines.[40] The first form, GlyH1, involving a protonated amine terminus gives rise to several intramolecular hydrogen bonds and, thus, a globular structure (Figure 1a), and the second form, GlyH2, with a protonated amide carbonyl oxygen, also results in intramolecular hydrogen bonding, but with retention of a somewhat more linear structure (Figure 1b).

The intensities of the parent and the successively increasing deuterated species in the H/D exchange experiment of protonated triglycine and ND_3 are shown as a function of reaction time in Figure 2. The virtually simultaneous appearance of the first three H/D exchanged species suggests that the lifetime of the initially formed adduct between the protonated peptide and ND_3 is sufficiently long that a single collision event can result in many reversible hydrogen transfers at the amine terminus generating the complex early time behavior. Modeling of the exchange rate constants gives results in good agreement with those obtained by Beauchamp and co-workers, in which the first three exchanges all occur at or near the collision rate constant (1.34×10^{-9} cm^3 molecule^{-1} s^{-1}) with each successive rate constant becoming slower. The d_3-to-d_4 exchange proceeds at roughly half of the collision rate, the d_4-to-d_5 exchange at 20% of the collision rate and, finally, the d_5-to-d_{6x} exchange at roughly 3% of the collision rate. As noted above, although the multiple H/D exchanges can be seen to occur and their rates determined, the mechanisms behind them are not immediately obvious. The computational study of the molecular structures and energetics of complexes of protonated triglycine and ND_3 is thus invaluable in the deduction of reaction mechanism.

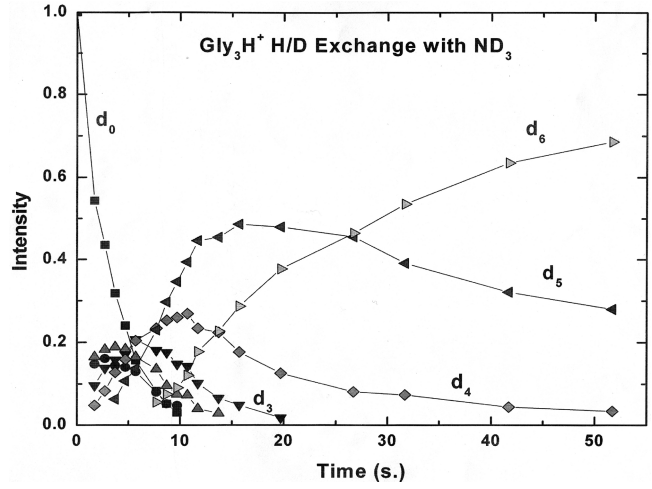

Figure 2. H/D exchange rate plot of protonated triglycine with ND_3. Six exchanges occur in total, and exchange is assumed to be sequential.

Initially, protonated triglycine was modeled to investigate the most energetically favorable structures in terms of Gibbs free energy. This information was used to find the most energetically

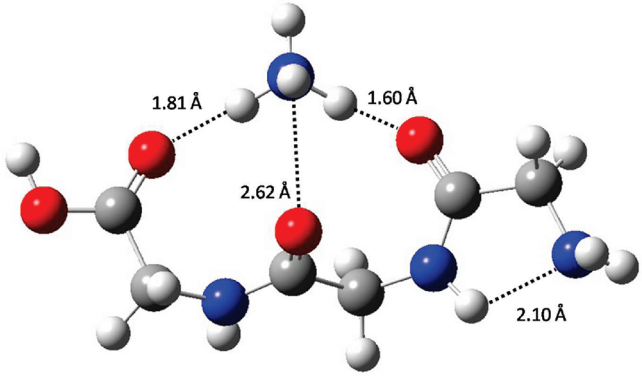

Figure 3. GlyHAm1.

favorable clusters with ND_3. GlyH2 is found to be the most stable isomer at the B3LYP level of theory, as previously discussed in a combined computational and infrared multiple photon dissociation (IRMPD) experimental study.[40] However, also as noted previously, GlyH1 is found to be the most stable structure when single point calculations at the MP2 level are performed. The IRMPD experimental data are thus best interpreted as being the result of a mixture of both of these two forms as the dominant species in an electrospray ionization ion trap mass spectrometer experiment. Therefore, any explanation of the gas phase H/D exchange experiments with ND_3 must consider that both GlyH1 and GlyH2 may be present to lead to formation of complexes to effect the H/D exchange and that interaction with ammonia may effect the interconversion of GlyH1 and GlyH2.

Amino. Upon interaction with ND_3 the most stable complex of the resulting adduct with protonated triglycine is found to be GlyHAm1 (Figure 3), which can be thought of most simply as arising from a nominally endothermic proton transfer from GlyH2 to ammonia, followed by solvation of the ammonium ion by the peptide to form a tridentate hydrogen bonded motif. The first of these hydrogen bonds involves interaction between one of the hydrogens of the resulting ammonium ion and the N-terminal amide (amide1) carbonyl oxygen with an N−H···O contact of 1.6 Å. A second hydrogen bond also results from the interaction of another ammonium ion hydrogen with the carbonyl oxygen of the C-terminal carboxyl group with an N−H···O contact of 1.8 Å. Finally a third, albeit weaker, hydrogen bond results from the interaction of the remaining ammonium hydrogen with the C-terminal amide (amide2) carbonyl oxygen with an N−H···O contact of 2.6 Å. It should be noted, however, that in the process, the hydrogen bond between the amide2 hydrogen and carbonyl oxygen at the C-terminus is lost. Although GlyHAm1 is the most stable adduct structure on the potential energy surface, it is not immediately obvious how this structure will lead to exchange of the labile hydrogens of protonated triglycine. Rather, it is instructive to examine the approach of an ammonia molecule to the two most stable structures of protonated triglycine.

The approach of ammonia to GlyH1 leads to a complex, GlyHAm2 (Figure 4a), which preserves the intramolecular hydrogen bonding motif of the peptide. In this structure, ammonia is bound by 86.5 kJ/mol. This interaction energy is sufficient to activate the complex, leading to rupture of the existing intramolecular hydrogen bond, followed by internal rotations, giving rise to the new complex, GlyHAE1 (Figure 4b), which can now be considered to be the starting point to explain H/D exchange of the amino hydrogens. GlyHAE1 has an ammonia binding energy of 91 kJ/mol. This initial complex

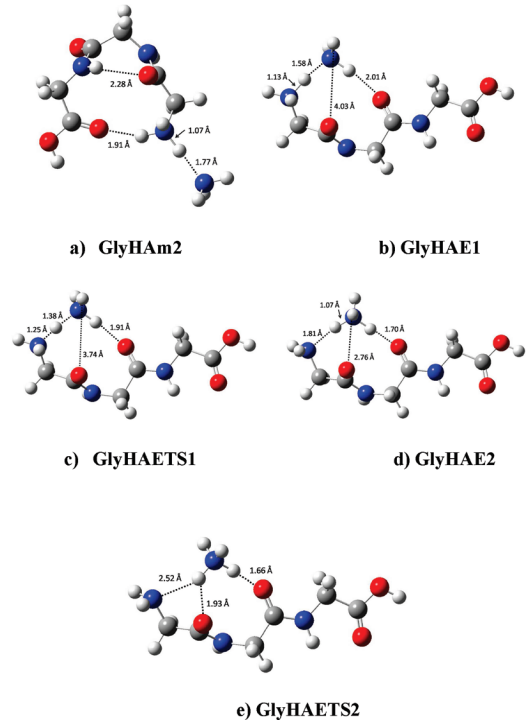

Figure 4

has undergone some notable geometric changes relative to the uncomplexed ammonium ion structure, GlyH1. Significantly, the N−H bond length of the bridging hydrogen bond has increased to 1.13 Å, compared with the 1.02−1.04 Å of the ammonium moiety in GlyH1. This, and the fact that the $N-H^+\cdots N$ distance to the attached ammonia molecule is 1.58 Å, indicate that a partial proton transfer is occurring in this new adduct structure. A second, albeit weaker, hydrogen bond from a hydrogen of the ammonia molecule to the carbonyl oxygen of amide2 is also apparent from the N−H···O contact of 2.01 Å.

The potential energy surface rationalizing H/D exchange of the amino hydrogens (Figure 5) exhibits a nearly-barrierless transition state to proton transfer, GlyHAETS1 (Figure 4c). This transition state exhibits an increased extent of proton transfer from the protonated amine terminus to ammonia with the N−H bond distance of the bridging proton to the amine nitrogen increasing to 1.25 Å, while the $N-H^+\cdots N$ contact to the ammonia molecule decreases to 1.38 Å. Simultaneously, the secondary hydrogen bond to the amide2 carbonyl also increases slightly, as exhibited by the decrease in the N−H···O contact to 1.91 Å. A slight rotation of the ammonia molecule is also evident as the contact from one of the ammonia hydrogens to the amide1 carbonyl oxygen decreases from 4.03 Å in the initial complex to 3.74 Å in the transition state.

Finally, a completion of the proton transfer leads to formation of an ammonium ion that benefits from considerably greater hydrogen bonding capabilities with other sites in the peptide chain, GlyHAE2 (Figure 4d), and in which ammonia is bound by only ∼11 kJ/mol less than that in the most stable complex. This improved hydrogen bonding situation is evident from the $N\cdots H^+-N$ distance of 1.81 Å from the nitrogen of the now neutral peptide to the bridging hydrogen and the much shorter $N-H^+\cdots N$ bond distance of 1.07 Å of the bridging hydrogen of the new ammonium ion. In addition, the proton transfer to generate an ammonium ion leads to greater positive charge on each of the ammonium ion hydrogens, thus facilitating additional interaction with other basic sites. This is shown by the now

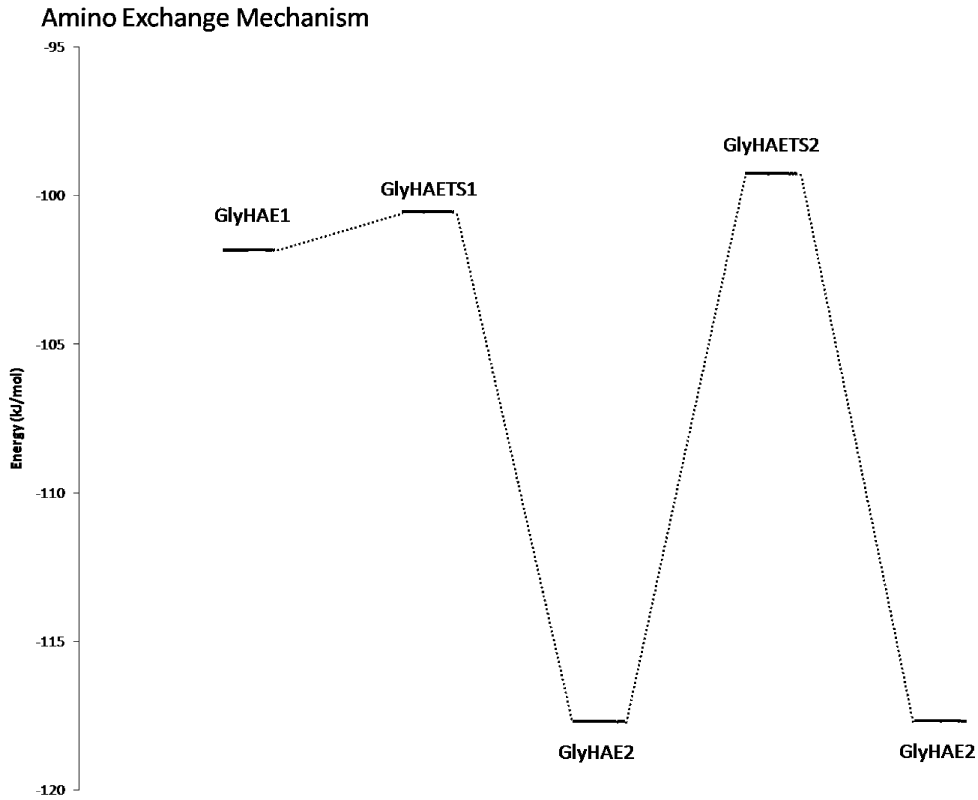

Figure 5. Potential energy surface for amino exchange mechanism.

shorter contact of 1.70 Å to the amide2 carbonyl oxygen and the substantially shorter contact of 2.76 Å to the amide1 carbonyl oxygen.

The final step in explaining exchange of the amine terminal hydrogens involves internal rotation of the ammonium ion to permute the hydrogen bound to the amine terminal nitrogen via a transition state, GlyHAETS2 (Figure 4e), which is only 17 kJ/mol above the minimum on the amino exchange surface, GlyHAE2, and still 99 kJ/mol lower than the energy of separated reactants. This internal rotation involves a rotation about an axis involving the hydrogen bond between the ammonium ion and the amide2 carbonyl oxygen. In the process, the hydrogen bond between the ammonium ion and the amino nitrogen lengthens as the hydrogen bonded hydrogen rotates out of the nearly linear (167°) axis of the bond. Simultaneously, a stronger hydrogen bond forms to the amide1 carbonyl oxygen by virtue of the closer approach of the hydrogen. Thus, the transition state also involves a tridentate hydrogen bonded structure. To complete the exchange mechanism, this rotation continues such that a formerly non-hydrogen bonding hydrogen of the ammonium ion rotates into a position to form a new hydrogen bond to the amino nitrogen, arriving at a structure energetically equivalent to GlyHAE2. This transition state allows for the reversible substitution of hydrogen for deuterium and, with a sufficiently long complex lifetime, the complete exchange of all three amine terminal hydrogens of the protonated triglycine can be rationalized, through the same mechanism, within a single collision event.

The overall amino hydrogen H/D exchange mechanism is shown schematically in Figure 5. The energy of separated reactants is taken to be 0 kJ/mol for this and all subsequent potential energy profiles. To more clearly depict transition states, this and subsequent potential energy profiles are presented as 0 K surfaces without inclusion of zero point energy. As shown previously,[41] this type of 0 K profile most clearly depicts the transition states on the surface, since inclusion of thermal and zero point energies as well as entropy, can result in transition states that are lower in enthalpy or free energy than the associated stable minima. Altough the enthalpies and free energies of the transition states will clearly play a role in the dynamics of the reactions, for purposes of clarity, the 0 K surfaces are preferable to identify these transition states. The 298 K enthalpies and free energies of each of the stationary points on the potential energy surface are therefore given in Table 1 and all subsequent tables depicting the exchange mechanisms.

TABLE 1: Relative Energetics, Amino Exchange Mechanism, Energetics of Separated Reactants Taken As Zero

structure	ΔE_{elec} (kJ/mol)	ΔH (kJ/mol) 298 K	ΔS (J/mol K) 298 K	ΔG (kJ/mol) 298 K
GlyHAE1	−101.8	−91.0	−127.4	−53.0
GlyHAETS1	−100.6	−98.1	−137.6	−57.1
GlyHAE2	−117.7	−103.9	−136.6	−63.2
GlyHAETS2	−99.3	−88.1	−136.8	−47.4

Amide1. The entry onto the potential energy surface for the exchange at the amide1 nitrogen can be considered to be the approach of ammonia to the amide1 hydrogen of GlyH1, which results in the complex GlyHAd1E1 (Figure 6a). This complex has an ammonia binding energy of ∼51 kJ/mol and exhibits an intramolecular hydrogen bond between a hydrogen of the protonated amine and the carbonyl oxygen of amide1 with a slightly elongated N−H bond distance of 1.08 Å and an $N-H^{+}\cdots O$ contact of 1.64 Å. The weaker bond to the ammonia molecule is demonstrated by the hydrogen bond distance of the hydrogen of the amide1 nitrogen to ammonia of 1.89 Å. In addition, a hydrogen of the ammonia molecule interacts with the carbonyl oxygen of the C-terminal carboxyl group with a contact of 2.19 Å.

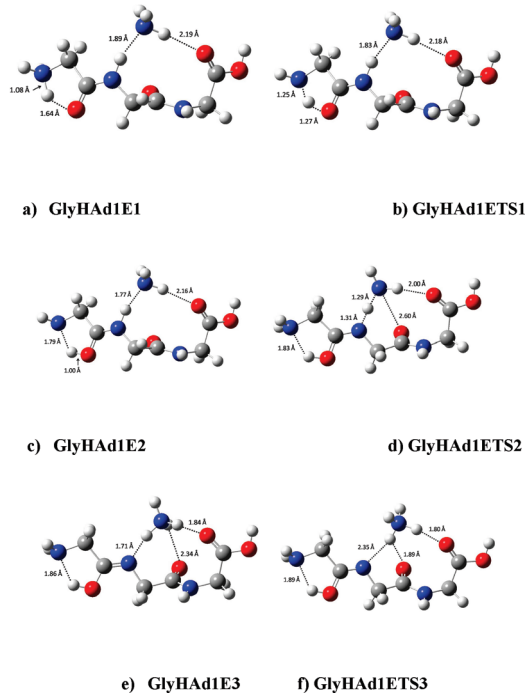

Figure 6

Subsequently, via a transition state, GlyHAd1ETS1 (Figure 6b), which is only ~6 kJ/mol higher in energy than its preceding structure, proton transfer commences from the nitrogen of the protonated amine terminus to the amide1 carbonyl oxygen. This transition state exhibits nearly equal N−H and O−H distances of 1.25 and 1.27 Å, respectively, indicating that in the transition state, this proton is nearly equally shared by these two heteroatoms. Only minor geometric changes take place in the remainder of the complex, the most significant of these being a reduction in the contact of the hydrogen of the amide1 nitrogen to ammonia to 1.83 Å.

Completion of this first intramolecular proton transfer results in a complex, GlyHAd1E2 (Figure 6c), that exhibits an ammonia binding energy ~10 kJ/mol higher than that of GlyHAd1E1. This completed proton transfer can be seen from the new O−H bond distance of 1.0 Å in what is effectively an imidol tautomer, with an intramolecular hydrogen bond to the terminal amine nitrogen of 1.79 Å. In addition, the contact of the hydrogen on the nitrogen of amide1 to ammonia decreases somewhat more to 1.77 Å. The contact of the hydrogen of ammonia to the carbonyl oxygen of the C-terminus decreases by a very minor extent to 2.16 Å.

This resulting complex similarly undergoes a nominally endothermic proton transfer from the amide1 nitrogen to ammonia via a low-lying transition state, GlyHAd1ETS2 (Figure 6d). This transition state again shows quite similar hydrogen bond contacts, with that from the amide1 nitrogen to the transferring proton of 1.31 Å and that from the same proton to the ammonia nitrogen of 1.29 Å. In addition, the contact of one of the ammonia hydrogens to the C-terminal carbonyl oxygen decreases to 2.0 Å, and a new interaction results from a twisting of the peptide chain coupled with a rotation of the ammonia molecule to lead to a second contact between an ammonia hydrogen and the carbonyl oxygen of amide2 of 2.6 Å.

Completion of the proton transfer yields a complex in which an ammonium ion is intramolecularly hydrogen-bonded simultaneously to the amide1 nitrogen, the carbonyl oxygen of the C-terminus, and the amide2 carbonyl oxygen, GlyHAd1E3 (Figure 6e), with hydrogen bond distances of 1.71, 1.84, and 2.34 Å, respectively. This complex is essentially identical in energy to GlyHAd1E2. A minor change is noted in the hydrogen bond distance between the amine nitrogen and the hydrogen of the protonated amide1 oxygen, which has slightly lengthened from the transition state, 1.83 Å, to the final product, 1.86 Å.

In analogous fashion to H/D exchange mechanism of the amino hydrogens, this species may permute the hydrogens of the ammonium ion via transition state GlyHAd1ETS3 (Figure 6f) to complete the exchange of the amide1 hydrogen. The formation of this transition state proceeds via a rotation about the hydrogen bond between the ammonium ion and the carbonyl oxygen of the carboxy terminus. In the course of this rotation, the hydrogen bond from the ammonium ion to the amide1 nitrogen increases in length, and the movement of this hydrogen-bonding hydrogen brings it in close approach to the amide2 carbonyl oxygen. The long contact (2.34 Å) to another hydrogen of the ammonium ion rotates out of interaction with this carbonyl oxygen. To effect H/D exchange, the final structure brings a formerly noninteracting hydrogen of the ammonium ion into a hydrogen bond with the amide1 nitrogen. The complete sequence of events to explain H/D exchange of the amide1 hydrogen is shown schematically in Figure 7. The 298 K energetics of each of the stationary points on the potential energy surface are given in Table 2.

Amide2. A mechanism for the amide2 H/D exchange involving the amine protonated triglycine is outlined in the Supporting Information. As shown there, the final exchange transition state appears to lie above the energy of separated reactants and, thus, appears not to be a viable means of exchange at this site. Since a mechanism to explain the amide2 exchange involving amine protonated triglycine appears not to be feasible, an alternative mechanism beginning with the amide1 carbonyl oxygen protonated species, GlyH2, can be considered. The approach of ammonia to the amide2 hydrogen induces a spontaneous transfer of the proton from the amide1 carbonyl oxygen to the amide2 carbonyl oxygen to form the structure GlyHAd2E1 (Figure 8a), involving ammonia now hydrogen-bonded to the amide2 N−H moiety. This new hydrogen bond geometry resembles strongly that found in GlyHAd2E1′ with the ammonia N−H and amine N−H bond distances differing by only 0.01 Å in each case. However, the secondary hydrogen bond formed from another ammonia hydrogen to the carbonyl oxygen of the carboxyl group is considerably shorter at 2.26 Å compared with the 2.43 Å of the analogous hydrogen bond in GlyHAd2E1′. Consequently, the enthalpy of GlyHAd2E1 is 16.7 kJ/mol more favorable than that of GlyHAd2E1′.

The subsequent step in this amide2 exchange mechanism involves proton transfer from the amide2 nitrogen to the approaching ammonia molecule. The transition state for this process, GlyHAd2ETS1 (Figure 8b), has an amide2 N−H distance of 1.42 Å and an ammonia N−H bond distance for the transferring proton of 1.20 Å, indicating that substantial proton transfer has occurred in the transition state. It is of interest to note the changes simultaneously occurring in the two other intramolecular hydrogen bonds in the system. The hydrogen bond of the ammonia hydrogen interacting with the carbonyl oxygen of the carboxyl terminus contracts from 2.26 to 1.97 Å, and the hydrogen bond between the two amide carbonyl oxygens involves a lengthening of the amide1 O−H distance from 1.38 to 1.54 Å and a contraction of the amide2 O−H distance from 1.08 to 1.02 Å.

The product of this proton transfer process results in a structure, GlyHAd2E2 (Figure 8c), with an amide N−H bond

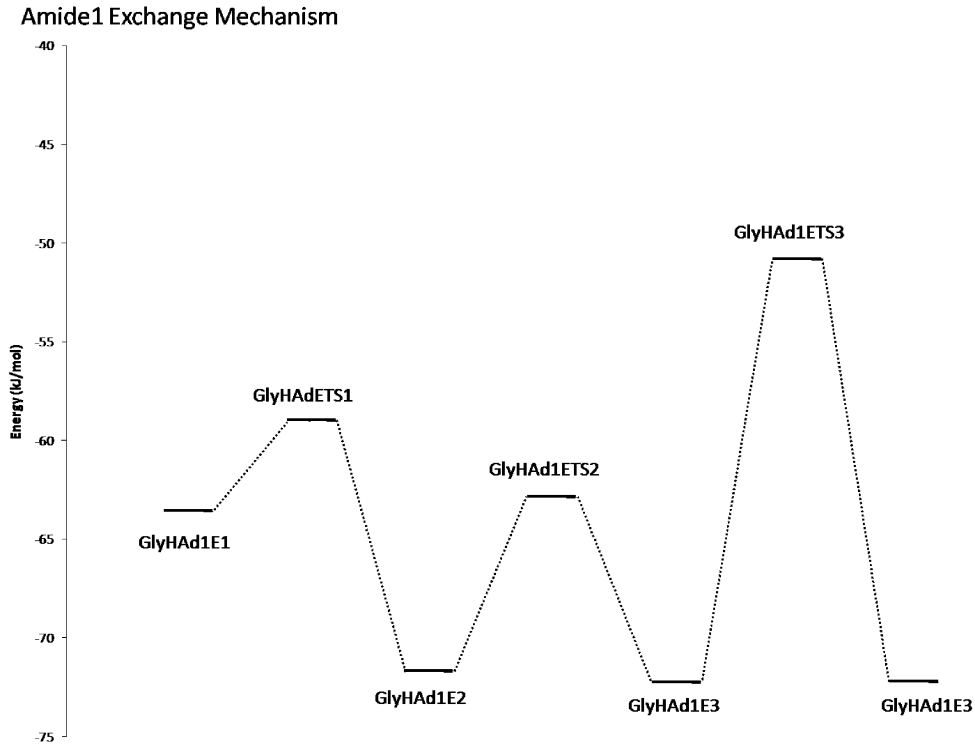

Figure 7. Potential energy surface for amide1 exchange mechanism.

TABLE 2: Relative Energetics, Amide1 Exchange Mechanism, Energetics of Separated Reactants Taken As Zero

structure	ΔE_{elec} (kJ/mol)	ΔH (kJ/mol) 298 K	ΔS (kJ/mol) 298 K	ΔG (kJ/mol) 298 K
GlyHAd1E1	−63.6	−51.5	−116.3	−16.8
GlyHAd1ETS1	−59.0	−57.6	−129.2	−19.1
GlyHAd1E2	−71.7	−61.4	−121.0	−25.3
GlyHAd1ETS2	−62.8	−63.7	−138.7	−22.3
GlyHAd1E3	−72.2	−61.0	−135.8	−20.5
GlyHAd1ETS3	−50.8	−40.9	−138.2	0.3

distance of 1.56 Å and an ammonia N−H distance to the transferred proton of 1.13 Å. The secondary hydrogen bond from ammonia to the carbonyl oxygen of the carboxyl terminus has similarly undergone additional contraction to 1.90 Å. This stable ammonium ion adduct has an enthalpy that is 24.2 kJ/mol more stable than the analogous species, GlyHAd2E3′, of the amine protonated amide2 exchange mechanism.

The H/D exchange transition state, GlyHAd2ETS2 (Figure 8d), involves a rotation of the ammonium ion moiety to produce

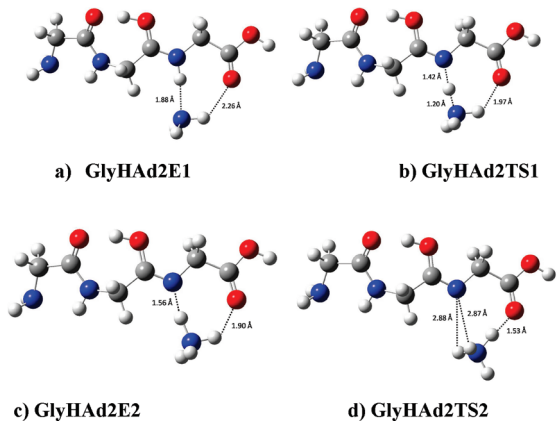

a) GlyHAd2E1 b) GlyHAd2TS1

c) GlyHAd2E2 d) GlyHAd2TS2

Figure 8

a species in which the primary hydrogen bond of the ammonium ion occurs to the carbonyl oxygen of the carboxyl terminus with an N−H bond distance of 1.08 Å and an O−H bond distance of 1.30 Å. The contacts of the amide2 nitrogen to the two closest hydrogens of the ammonium ion are 2.88 and 2.87 Å. Interestingly, the hydrogen bond between the two amide carbonyl oxygens also undergoes a slight change, with an amide1 O−H distance of 1.61 Å and an amide2 O−H distance of 1.01 Å. Thus, the amide2 H/D exchange can be seen to be readily achieved via this mechanism involving the amide1 carbonyl oxygen protonated species, GlyH2. The complete sequence of events to explain H/D exchange of the amide2 hydrogen is shown schematically in Figure 9. The 298 K energetics of each of the stationary points on the potential energy surface are given in Table 3.

Carboxyl. All attempts to devise a mechanism for exchange of the C-terminal hydroxyl hydrogen beginning with the amine protonated species, GlyH1, also failed to yield effective interaction of ammonia with the hydroxyl hydrogen, since the intramolecular hydrogen bond between the amine and carboxyl termini leads instead to interaction of ammonia with the protonated amine hydrogens. The exchange of the C-terminal hydroxyl hydrogen is best rationalized, therefore, via formation of a complex between the amide carbonyl protonated triglycine, GlyH2, and ammonia. The complex initially formed involves a hydrogen bond between the hydrogen of the C-terminal hydroxyl group and the ammonia nitrogen, GlyHCE1 (Figure 10a). It is interesting to note that although the backbone structure of the protonated peptide moiety remains relatively unperturbed during complex formation with ammonia, an intramolecular proton transfer from amide1 carbonyl oxygen to amide2 carbonyl oxygen actually accompanies the addition of ammonia at the C-terminus. The O−H−O interaction of the carbonyl protonated peptide, GlyH2, changes from an amide1 oxygen to a hydrogen distance of 1.06−1.37 Å in the newly formed ammonia complex. Simultaneously, the previous hydrogen to amide2

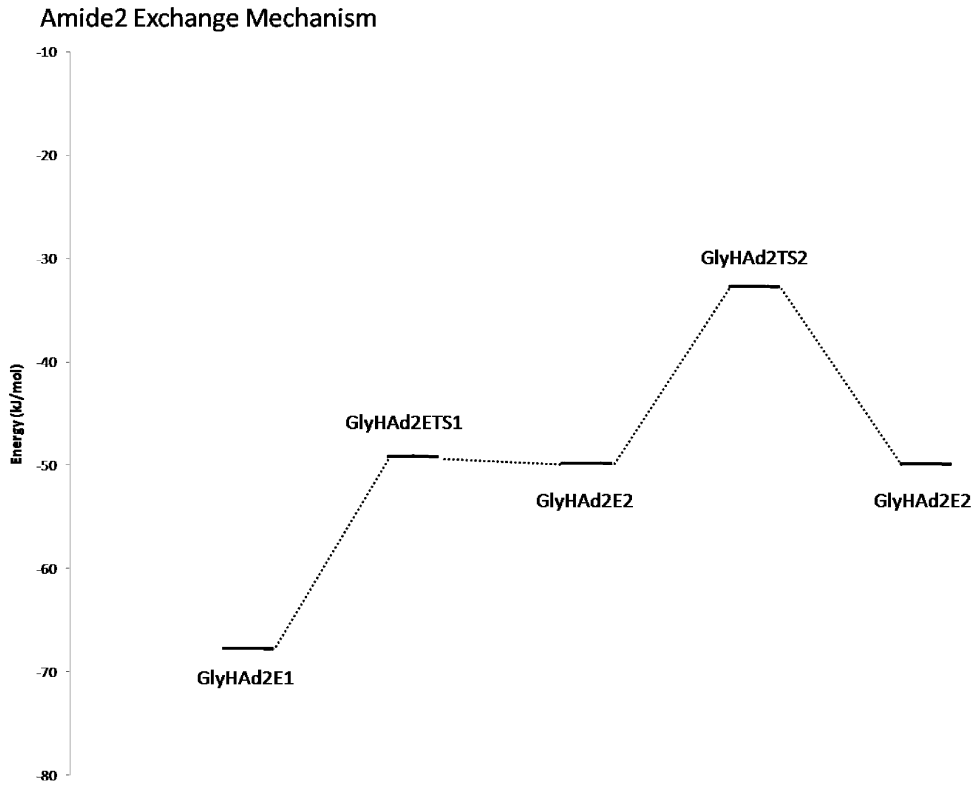

Figure 9. Potential energy surface for amide2 exchange mechanism.

TABLE 3: Relative Energetics- Amide2 Exchange Mechanism- Energetics of Separated Reactants Taken As Zero

structure	ΔE_{elec} (kJ/mol)	ΔH (kJ/mol) 298 K	ΔS (kJ/mol) 298 K	ΔG (kJ/mol) 298 K
GlyHAd2E1	−67.7	−62.8	−114.0	−28.8
GlyHAd2ETS1	−49.0	−51.2	−136.7	−10.4
GlyHAd2E2	−49.9	−44.3	−126.7	−6.6
GlyHAd2ETS2	−32.8	−25.6	−133.0	14.0

carbonyl oxygen contact of 1.42 Å in GlyH2 now becomes a covalent bond of 1.08 Å in the ammonia complex. Interestingly, the O−H−O bond angle changes only minimally going from 164° to 166° from GlyH2 to GlyHCE1. The newly formed ammonia complex has an amide1 N−H distance of 1.02 Å, with an interaction with the carbonyl oxygen of the C-terminus of 2.03 Å. The hydrogen bond to ammonia via the hydroxyl group has a O−H···N contact of 1.57 Å and a slightly elongated O−H bond distance of 1.05 Å.

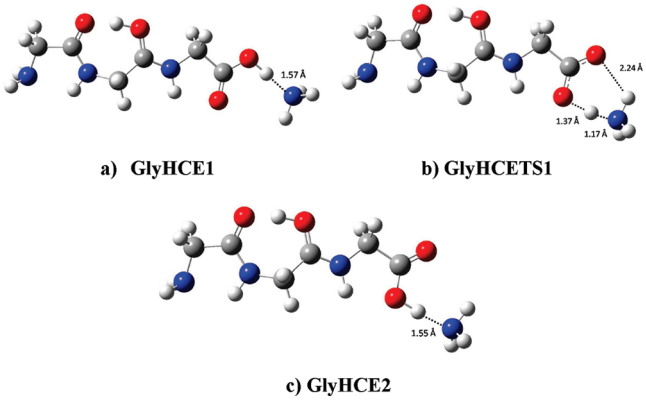

Figure 10

Subsequently, GlyHCE1 proceeds to a transition state, GlyHCETS1 (Figure 10b), in which the hydroxyl hydrogen of the C-terminus has undergone substantial transfer as a proton to ammonia, and the resulting ammonium ion bends to facilitate a hydrogen bond interaction between a second ammonium N−H and the carbonyl oxygen of the C-terminal carboxyl group. This species has a relatively long contact of 2.24 Å from the formerly hydroxyl oxygen to the transferred hydrogen now bonded to ammonia. The newly formed hydrogen bond between the formerly carbonyl oxygen and the ammonium nitrogen involves an O−H bond distance of 1.37 Å and an N−H bond distance of 1.17 Å.

This species then leads to facile proton transfer from ammonium ion to the carbonyl oxygen with a new O−H bond distance of 1.06 Å and an N−H bond distance of 1.55 Å. This species, GlyHCE2 (Figure 10c), also now has a long contact of 2.79 Å between a second hydrogen of the ammonia and the new carbonyl oxygen. As a result of the doubly hydrogen-bonded geometry of the transition state, this mechanism has effectively carried out H/D exchange by virtue of the fact that the hydrogen back-donated is different from the hydrogen initially abstracted. The complete sequence of events to explain H/D exchange of the carboxyl hydrogen is shown schematically in Figure 11. The 298 K energetics of each of the stationary points on the potential energy surface are given in Table 4.

Betaine. Betaine has been used previously as a model in the investigation of H/D exchange by Beauchamp et al. to better understand the exchange of its sole labile hydrogen, the carboxyl proton. In comparable fashion, the mechanism has been investigated in the present work and, not surprisingly, has been found to be quite analogous to that determined here for the exchange of the carboxyl hydrogen in protonated triglycine. The H/D exchange can be thought of as being initiated by the approach of ammonia to protonated betaine in its most stable configuration, which places the O−H moiety trans to the C−N

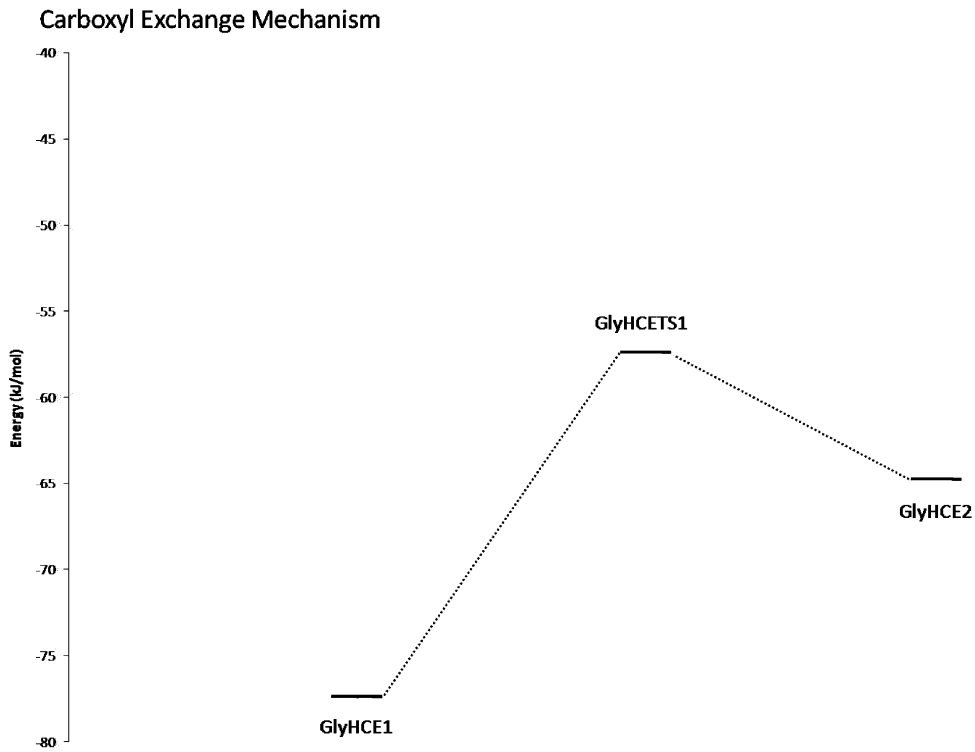

Figure 11. Potential energy surface for carboxyl exchange mechanism.

TABLE 4: Relative Energetics, Carboxyl Exchange Mechanism, Energetics of Separated Reactants Taken As Zero

structure	ΔE_{elec} (kJ/mol)	ΔH (kJ/mol) 298 K	ΔS (kJ/mol) 298 K	ΔG (kJ/mol) 298 K
GlyHCE1	−77.4	−74.9	−116.9	−40.1
GlyHCETS1	−57.4	−58.8	−142.0	−16.5
GlyHCE2	−64.7	−63.0	−116.0	−28.5

bond. The initially formed ammonia adduct, BetHCE1 (Figure 12a), has a hydrogen bond distance from the ammonia nitrogen to the carboxyl hydrogen of 1.52 Å, which is slightly less than that observed in GlyHCE1. This is consistent with the greater binding enthalpy of 84.6 kJ/mol for the betaine adduct.

The system then proceeds through a transition state, BetHCETS1 (Figure 12b), in which an ammonium ion moiety interacts with the zwitterionic betaine structure with O−H contacts of 1.58 and 1.98 Å. At the same time, the respective N−H bond distances are 1.09 and 1.04 Å, indicating that this is very much an ammonium ion.

To complete the H/D exchange, the ammonium ion then transfers a proton to the formerly carbonyl oxygen with an O−H bond length of 1.08 Å and a hydrogen bond to ammonia of 1.50 Å. This species resulting from the H/D exchange, BetHCE2 (Figure 12c), is 10 kJ/mol less favorable than the starting structure, which is largely the result of the greater stability of protonated betaine itself in which the O−H moiety and the trimethylamine moiety exist in a trans configuration. By comparison, the two different conformers of protonated betaine differ in stability by 10 kJ/mol. The complete sequence of events to explain H/D exchange of the amide1 hydrogen is shown schematically in Figure 13. The 298 K energetics of each of the stationary points on the potential energy surface are given in Table 5.

The relative energetics of the several mechanisms outlined here would lead to the prediction that the relative rates of H/D

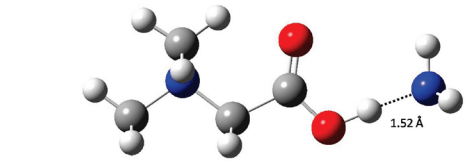

a) BetHCE1

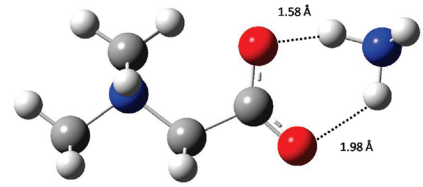

b) BetHCETS

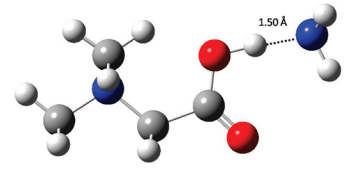

c) BetHCE2

Figure 12

exchange would be in the order: amine terminus > carboxyl terminus > amide1 > amide2. It is clear from the fact that the first three exchanges occur virtually simultaneously that the amine terminal hydrogens are, indeed, the most rapidly exchanged. Some insight into which hydrogen is the second most easily exchanged may be gained from the observation of Beauchamp et al. that sodiated polyglycines exchange only three hydrogens, presumably those at the amine terminus and carboxyl terminus.[30] It can be expected, then, that the carboxyl terminus hydrogens are the second most rapidly exchanged in the

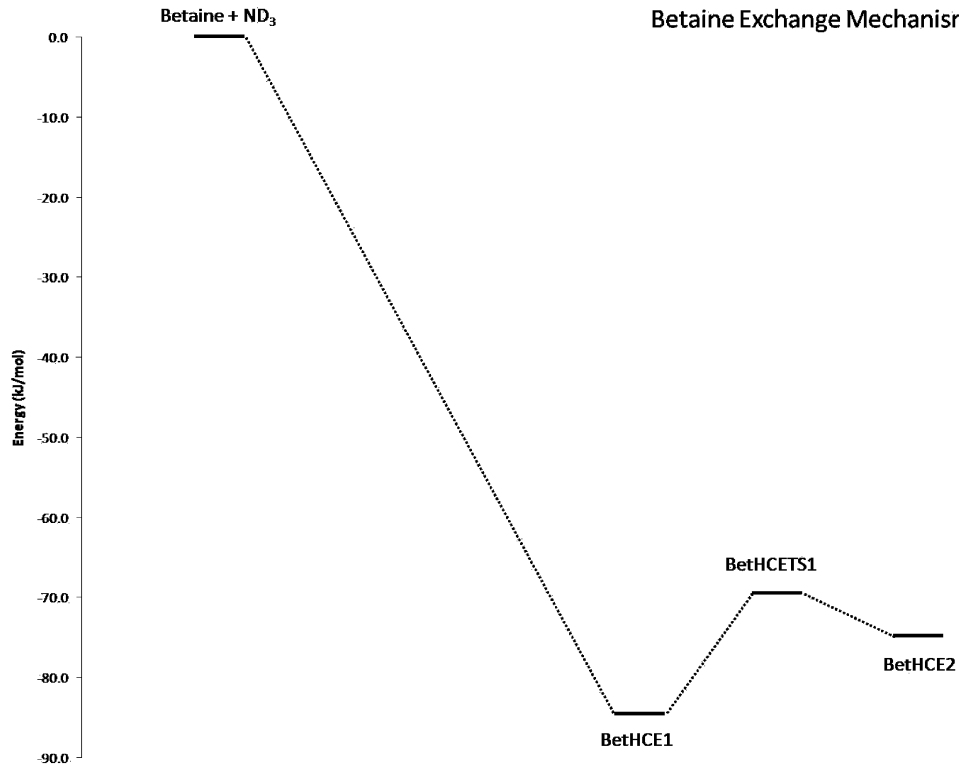

Figure 13. Potential energy surface for betaine carboxyl exchange mechanism.

TABLE 5: Relative Energetics, Betaine Carboxyl Exchange Mechanism, Energetics of Separated Reactants Taken As Zero

structure	ΔE_{elec} (kJ/mol)	ΔH (kJ/mol) 298 K	ΔS (kJ/mol) 298 K	ΔG (kJ/mol) 298 K
BetHCE1	−88.0	−84.6	−118.3	−49.4
BetHCETS1	−73.3	−69.4	−149.6	−24.8
BetHCE2	−77.7	−74.6	−119.5	−39.0

protonated species. Similarly, the fact that the amide hydrogens do not exchange in sodiated polyglycines is consistent with the most energetically demanding mechanisms elucidated here for the protonated polyglycines.

Conclusion

Although the H/D exchange mechanisms outlined above bear qualitative similarities to those proposed by Beauchamp and co-workers in the initial study of H/D mechanisms of protonated polyglycines, the intimate details revealed here show considerable additional complexity. The onium ion mechanism in that work involved formation of a complex in which proton transfer occurs to ammonia and the resulting ammonium ion undergoes multiple hydrogen bonding interactions with several basic sites of the peptide chain. This is consistent with the mechanism proposed in the present work (Figure 5) for exchange of the amine terminal hydrogens in which an intermediate, GlyHAE2, is implicated involving an ammonium ion that simultaneously undergoes hydrogen bonding interactions with the amine terminal nitrogen and the two carbonyl oxygens.

The salt bridge mechanism proposed by Beauchamp for exchange at the carboxyl terminus is also somewhat similar to the mechanism proposed here in Figure 11 as well as the mechanism of the single betaine exchange (Figure 13). The substantive difference is that it was necessary in the present study to invoke association of ammonia with the terminal hydroxyl of the C-terminus of the carbonyl protonated form of protonated triglycine, GlyH2. In contrast, all attempts to model the carboxyl exchange starting from association of ammonia with the hydroxyl hydrogen of the amine protonated form, GlyH1, lead to transfer of ammonia to the amine terminus because of the proximity of the terminal ammonium ion in the intramolecular hydrogen bond between the protonated amine terminus and the C-terminal carbonyl oxygen.

Finally, the tautomer mechanism of Beauchamp's work also bears a similarity to that proposed here for the exchanges of both amide hydrogens. In the case of amide1, an intramolecular proton transfer results in protonation of the amide1 carbonyl oxygen, and approach of ammonia to the amide1 N−H results in proton transfer to give an ammonium ion interacting with an imido nitrogen of the amide1 moiety (Figure 7). Similarly, the mechanism for H/D exchange at amide2 (Figure 9) involves a tautomeric species, the difference being that this mechanism is initiated from the amide1 carbonyl oxygen protonated triglycine. In the course of this mechanism, another tautomer does result, GlyHAd2E2, in which an ammonium ion interacts with the imido nitrogen of the tautomer of amide2.

The present work provides quantitative validation and detailed structural information for gas phase H/D exchange of protonated triglycine with ND_3 as the exchange reagent. More importantly, this work may serve as a conceptual model for gas phase H/D exchange of protonated peptides in general.

Acknowledgment. The generous financial support by the Natural Sciences and Engineering Research Council of Canada (NSERC) is gratefully acknowledged. B.E.Z. was also supported in part by the University of Waterloo from the Undergraduate Research Internship Program. B.E.Z. acknowledges the assistance and support received from R. Marta, J. Martens, and R. Wu. In addition, T.B.M. acknowledges the hospitality of G. Ohanessian and Laboratoire DCMR at Ecole Polytechnique (France) where the FT-ICR experiments were performed.

Supporting Information Available: Additional information as noted in text and complete ref 34. This material is available free of charge via the Internet at http://pubs.acs.org.

References and Notes

(1) Englander, S. W. *Science* **1993**, *262*, 848.
(2) Parker, M. J.; Clarke, A. R. *Biochemistry* **1997**, *36*, 5786.
(3) Nishimura, C.; Dyson, H. J.; Wright, P. E. *Proc. Natl. Acad. Sci.* **2005**, *102*, 4765.
(4) Uzawa, T.; Nishimura, C.; Akiyama, S.; Ishimori, K.; Takahashi, S.; Dyson, H. J.; Wright, P. E. *Proc. Natl. Acad. Sci.* **2008**, *105*, 13859.
(5) Mobley, J. A.; Poliakov, A. *Protein Sci.* **2009**, *18*, 1620.
(6) Maity, H.; Lim, W. K.; Rumbley, J. N.; Englander, S. W. *Protein Sci.* **2003**, *12*, 153.
(7) Ghaemmaghami, S.; Fitzgerald, M. C.; Oas, T. G. *Proc. Natl. Acad. Sci.* **2000**, *97*, 8296.
(8) Wang, F.; Tang, X. J. *Biochemistry* **1996**, *35*, 4069.
(9) Yan, X. G.; Watson, J.; Ho, P. S.; Deinzer, M. L. *Mol. Cell. Proteomics* **2004**, *3*, 10.
(10) Wang, F.; Li, W. Q.; Emmett, M. R.; Hendrickson, C. L.; Marshall, A. G.; Zhang, Y. L.; Wu, L.; Zhang, Z. Y. *Biochemistry* **1998**, *37*, 15289.
(11) Busenlehner, L. S.; Armstrong, R. N. *Arch. Biochem. Biopyhys.* **2005**, *433*, 34.
(12) Demmers, J. A. A.; Haverkamp, J.; Heck, A. J. R.; Koeppe, R. E.; Killian, J. A. *Proc. Natl. Acad. Sci.* **2000**, *97*, 3189.
(13) Demmers, J. A. A.; van Duijn, E.; Haverkamp, J.; Greathouse, D. V.; Koeppe, R. E.; Heck, A. J. R.; Killian, J. A. *J. Biol. Chem.* **2001**, *276*, 34501.
(14) Yamaguchi, K. I.; Katou, H.; Hoshino, M.; Hasegawa, K.; Naiki, H.; Goto, Y. *J. Mol. Biol.* **2004**, *338*, 559.
(15) Lu, X. J.; Wintrode, P. L.; Surewicz, W. K. *Proc. Natl. Acad. Sci.* **2007**, *104*, 1510.
(16) Toyama, B. H.; Kelly, M. J. S.; Gross, J. D.; Weissman, J. S. *Nature* **2007**, *449*, 233.
(17) Nazabal, A.; Hornemann, S.; Aguzzi, A.; Zenobi, R. *J. Mass Spectrom.* **2009**, *44*, 965.
(18) Glickson, J. D.; Mayers, D. F.; Settine, J. M.; Urry, D. W. *Biochemistry* **1972**, *11*, 477.
(19) Craven, C. J.; Derix, N. M.; Hendriks, J.; Boelens, R.; Hellingwerf, K. J.; Kaptein, R. *Biochemistry* **2000**, *39*, 14392.
(20) Hoshino, M.; Katou, H.; Hagihara, Y.; Hasegawa, K.; Naiki, H.; Goto, Y. *Nat. Struct. Biol.* **2002**, *9*, 332.
(21) Whittemore, N. A.; Mishra, R.; Kheterpal, I.; Williams, A. D.; Wetzel, R.; Serpersu, E. H. *Biochemistry* **2005**, *44*, 4434.
(22) Zhang, Z. Q.; Smith, D. L. *Protein Sci.* **1993**, *2*, 522.
(23) Cheng, X. H.; Fenselau, C. *Int. J. Mass Spectrom. Ion Processes* **1992**, *122*, 109.
(24) Gard, E.; Willard, D.; Bregar, J.; Green, M. K.; Lebrilla, C. B. *Org. Mass Spectrom.* **1993**, *28*, 1632.
(25) Gard, E.; Green, M. K.; Bregar, J.; Lebrilla, C. B. *J. Am. Soc. Mass Spectrom.* **1994**, *5*, 623.
(26) Wood, T. D.; Chorush, R. A.; Wampler, F. M.; Little, D. P.; O'Connor, P. B.; McLafferty, F. W. *Proc. Natl. Acad. Sci.* **1995**, *92*, 2451.
(27) Wyttenbach, T.; Bowers, M. T. *J. Am. Soc. Mass Spectrom.* **1999**, *10*, 9.
(28) Rozman, M. *J. Am. Soc. Mass Spectrom.* **2005**, *16*, 1846.
(29) Polfer, N. C.; Dunbar, R. C.; Oomens, J. *J. Am. Soc. Mass Spectrom.* **2007**, *18*, 512.
(30) Cox, H. A.; Julian, R. R.; Lee, S. W.; Beauchamp, J. L. *J. Am. Chem. Soc.* **2004**, *126*, 6485.
(31) Rozman, M.; Bertosa, B.; Klasinc, L.; Srzic, D. *J. Am. Soc. Mass Spectrom.* **2006**, *17*, 29.
(32) Campbell, S.; Rodgers, M. T.; Marzluff, E. M.; Beauchamp, J. L. *J. Am. Chem. Soc.* **1995**, *117*, 12840.
(33) Correia, C. F.; Balaj, P. O.; Scuderi, D.; Maitre, P.; Ohanessian, G. *J. Am. Chem. Soc.* **2008**, *130*, 3359.
(34) Frisch, M. J.; Trucks, G. W.; Schlegel, H. B.; . *Gaussian 03*, Gaussian Inc.: Wallingford, CT, 2004.
(35) Becke, A. D. *J. Chem. Phys.* **1993**, *98*, 5648.
(36) Stephens, P. J.; Devlin, F. J.; Chabalowski, C. F.; Frisch, M. J. *J. Phys. Chem.* **1994**, *98*, 11623.
(37) Scott, A. P.; Radom, L. *J. Phys. Chem.* **1996**, *100*, 16502.
(38) Delbene, J. E.; Person, W. B.; Szczepaniak, K. *J. Phys. Chem.* **1995**, *99*, 10705.
(39) Wang, P.; Wesdemiotis, C.; Kapota, C.; Ohanessian, G. *J. Am. Soc. Mass Spectrom.* **2007**, *18*, 541.
(40) Wu, R. H.; McMahon, T. B. *J. Am. Chem. Soc.* **2007**, *129*, 11312.
(41) Wu, R. H.; McMahon, T. B. *Can. J. Chem.* **2005**, *83*, 1978.

JP105170F